Characterization and Linearization of High Bandwidth Integrated Optical Transmitter Modules

Markus Nölle(1), M. Sezer Erkılınç(2), Robert Emmerich(2), Carsten Schmidt-Langhorst(2), Robert Elschner(2) , and Colja Schubert(2)

(1) HTW Berlin, University of Applied Sciences, Wilhelminenhofstraße 75A, 12459 Berlin, Germany, markus.noelle@htw-berlin.de

(2) Fraunhofer Institute for Telecommunications, HHI, Einsteinufer 37, 10587 Berlin, Germany

Abstract Linearization of a high-bandwidth coherent driver module is demonstrated to enable the use of larger swing for driving signals. It is verified for symbol rates and modulation formats up to 80-GBd and 256-QAM, leading up to 3.7-dB higher transmitter output power compared to linear predistortion.

Introduction

Coherent technologies have become the choice of technology in data center interconnects (DCI) due to the increasing demand for bandwidth driven by cloud storage/computing applications. Symbol rates above 100 GBd are currently achievable using optical transmitters implemented with discrete, carefully selected components, such as driver amplifiers (DAs) and optical modulators[1]. Their performance can be further improved by employing additional digital signal processing (DSP) stages to mitigate residual linear[2] and nonlinear distortions induced by high-performance, yet non-deal components[3],[4]. Typically, the characteristics of such components are first measured individually, and subsequently, a nonlinear digital predistortion (NLPD) is performed[5]. However, due to cost and space requirements, the industry is highly in favor of integrated devices which makes such characterization approach eminently cumbersome.

The most recent available optical transmitter module, which co-packages a linear, quad-channel, differential driver with an InP dual-polarization (DP)-IQ modulator chip, is designed for 400 Gb/s systems using a DP 64-GBd 16-QAM signal, so-called high bandwidth coherent driver module (HB-CDM)[6]. However, the individual components used inside such integrated modules usually exhibit significantly enhanced distortions. Moreover, it is typically not possible to characterize the individual internal transmitter components since they are not individually accessible for measurements. Thus, the entire HB-CDM needs to be treated as a 'black-box' and the required optimum digital predistortion (DPD) must be derived from the (coherent) optical output signal of the HB-CDM. Demonstrations and performance investigations of such a predistortion concept have recently been demonstrated[7],[8].

In this work, we systemically characterize the system under test (SUT), i.e., by treating as a black-box to measure the linear and nonlinear effects of the integrated HB-CDM at various DA gain settings. Significant nonlinear distortions induced by larger DA gains and the subsequent optical modulator were observed which were mitigated using the proposed system identification (SI) in conjunction with the NLPD scheme reported in[5].

For a 64-GBd 64-QAM, it is shown that the NLPD increases the system performance for all investigated DA gains, while the improvement compared to sole linear predistortion increases for increasing DA gains. Thus, the proposed approach demonstrates the advantage of using NLPD as two-fold: It enables the use of higher DA gain settings and a larger swing of the modulator driving signals, resulting in 3.7 dB higher transmitter output power, and hence a higher transmitter OSNR. Further, it allows for an overall higher system performance characterized by the BER. We also demonstrate similar advantages for 64-GBd 256-QAM and 80-GBd 256-QAM, respectively.

Experimental setup

The experimental setup is shown in Fig. 1. It consists of two stages, namely SI followed by DPD, and performance assessment, as depicted in green and purple boxes, respectively. In both cases, the same experimental testbed was used whereas different DSP chains were employed to generate the electrical signals.

The optical signal was generated using an external cavity laser, operating at 1550 nm and 16 dBm. The SUT was a prototype of an HB-CDM-based Optical Multi-Format Transmitter (OMFT, by ID Photonics), consisting of a quad-channel differential DAs followed by a DP-IQ-modulator as shown in the red box in Fig.1. The integrated DAs were operated at different gains to perform the identification and performance evaluation using DPD. The waveforms were generated offline and uploaded to a 4-Ch 120-GSa/s arbitrary waveform generator (AWG) with 8-bit nominal amplitude

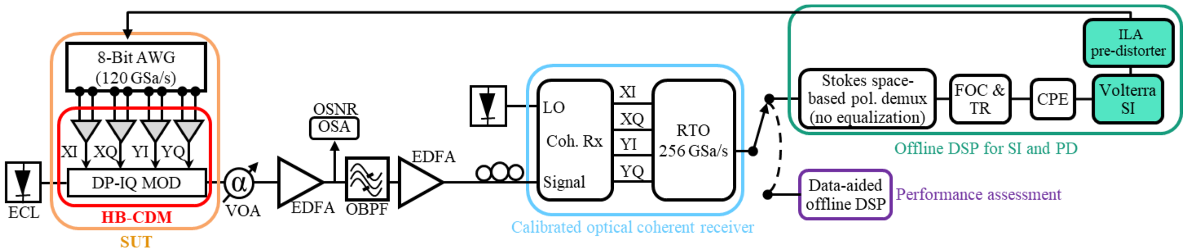

Fig. 1: Experimental setup used for system identification (SI) and DPD (green box) as well as for performance evaluation (purple box) of the integrated HB-CDM (red box). AWG: Arbitrary Waveform Generator. FOC: Frequency Offset Correction. TR: Timing Recovery. CPE: Carrier Phase Estimation. ILA: Indirect Learning Algorithm. LO: Local Oscillator.

resolution. At the receiver, the signal was detected and digitized using a calibrated optical coherent receiver (marked with a blue box), comprising a 70-GHz polarization- and phase-diverse receiver, followed by a 110-GHz 4-channel 256-GSa/s real-time oscilloscope.

For performance evaluation, 64-GBd 64-QAM, 80-GBd 64-QAM and 64-GBd 256-QAM signals were used to assess the effectiveness of the proposed DPD scheme. Following the bit-to-symbol mapping including a header insertion (CAZAC-64 training sequences[9], at ~1% overhead[10]), a root-raised cosine pulse-shaping filter with a roll-off factor of 0.1 was applied and the signals were resampled to 120-GS/s. Finally, the signal was predistorted, as described in the next section and uploaded to the AWG memory.

Since data-aided DSP operation was utilized for performance assessment, at the receiver DSP first data-aided frequency offset correction (FOC) and polarization demultiplexing were jointly performed[11] followed by a blind phase search carrier phase estimation (CPE)[12]. A 15-tap real-valued, T-spaced 4x4 MIMO time-domain equalizer was employed[13] prior to symbol decision. Finally, the pre-FEC BER was calculated over at least 2 million bits.

Transmitter identification and linearization

To identify distortions induced solely by the transmitter, we first calibrated the optical coherent receiver (frontend and scope) to compensate for the IQ-skew and frequency response. To perform the identification of the SUT (orange box in Fig. 1), a 96-GBd DP-16QAM 'probe' signal (with a roll-off factor of 0.01) was generated using 2^{15} random bit sequences. To determine the transmitter distortions for each quadrature independently, the four quadratures of the optical signal need to be separated yet performing no equalization at the receiver. Thus, the DSP steps of resampling, polarization separation in Stokes space[14], FOC[15], retiming, data-aided ('genie') CPE and normalization were performed on the received signal, respectively. The measured and demultiplexed quadratures and the transmitted reference quadratures were used to derive truncated, time-invariant third order Volterra kernels. The kernels therefore describe the linear and nonlinear distortions of the transmitter module for each quadrature. To obtain these kernels, a penalized least squares estimation[16] was used. Following the SI, a predistorting filter, which was trained using an indirect-learning architecture[17] (ILA), was generated to mitigate the nonlinearities caused by the module. The ILA procedure is extensively described in[5]. For comparison, we also trained linear predistortion (LPD) filters using a 512-tap memory as well as third-order NLPD filters with kernel memory lengths of 512, 9, 9 taps for different DA gain settings.

In our experiments, the gains of the DAs within the HB-CDM were adjusted ranging from 0 (lowest gain) to 255 (highest gain). To increase the modulator swing and yield a higher optical transmitter output power, it is preferable to choose a gain as large as possible. However, this typically causes increased nonlinear distortions, which limit the performance. Thus, we performed the above-described SI for various amplifier gains to quantify the nonlinear distortions and assessed the ability to mitigate these via NLPD. We found that the DAs behave linear up to a gain setting of 75 but start generating substantial nonlinear distortions above this gain setting.

Performance evaluation of the Linearization

To evaluate the performance of the characterization and DPD methods, we first investigated an optical system operating at 64-GBd 64-QAM (768 Gb/s gross data rate). Linearly and nonlinearly pre-distorted waveforms are used at two different gain settings, in which a gain of 75 corresponds to a (almost) linear operation point, and a gain of 120 introduces nonlinear distortions. At these two gain settings, the BER vs. OSNR for both LPD and NLPD cases are shown in Fig. 2 (a). The NLPD outperforms the LPD in all cases and the performance difference in general gets larger with increasing OSNR. For the lower amplifier gain setting (75, blue curves), the performance difference between the LPD and NLPD schemes is rather small (at most a factor of 1.5 in terms of BER). This result is intuitive since the module operates

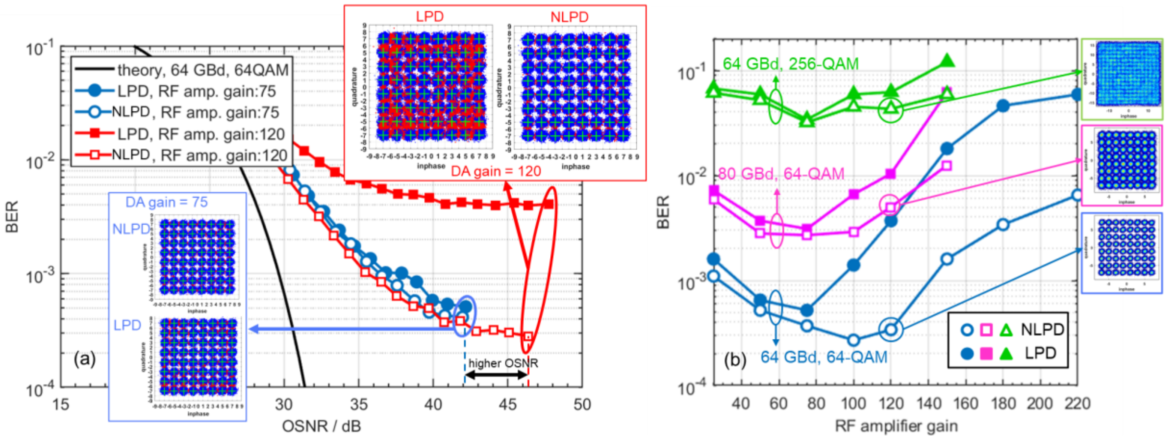

Fig. 2: (a) BER vs OSNR in 0.1 nm, blue curves (circular markers) correspond to a lower DA gain setting (75) whereas the red curves (squares) to a higher gain setting of 120. Blue inset shows the received constellations and the errors shown in red of the X polarization for the lower gain with LPD and NLPD, respectively. The red inset shows the constellations and errors for the higher gain setting. (b) BER as a function of the DA gain setting for various modulation formats (64-QAM and 256-QAM) and symbol rates (64 GBd and 80 GBd). Solid symbols represent the LPD case, while empty symbols mark the NLPD case.

in an (almost) linear regime, generating small nonlinear distortions, i.e., requiring marginal NLPD. This can also be observed in the blue inset of Fig. 2 (a) which shows the received constellations (blue points) of the X polarization together with the erroneous symbols (red points) for both DPD schemes at the highest achievable OSNR values. The slight improvement (from a BER of 4e-4 to 3e-4) is attributed to the mitigation of the modulator's nonlinear transfer function.

On the contrary, at the higher gain setting (120, red curves and squares), representing the nonlinear operation point, the NLPD performs about one order of magnitude better than the LPD for high OSNR values. The main reason is that LPD fails to mitigate the errors for the symbols severely distorted, in particular the outer (highest power) ones whereas NLPD successfully removes such distortions, as can be observed in the red inset.

The results evidently indicate that the DA within the HB-CDM must be set to a considerably lower gain for the LPD case to operate the system at a similar BER compared to the NLPD case. However, this operation point leads to a 3.7-dB lower optical output power, and hence, a lower achievable transmitter OSNR (marked with an arrow in Fig. 2 (a)).

Moreover, we investigated the performance of the NLPD for higher symbol rates and modulation orders by sweeping the DA gain settings. In Fig. 2 (b), the BER with respect to the amplifier gain is shown for the previously discussed system, as well as for a system employing a 64-QAM at 80-GBd (960 Gb/s gross data rate) and a 256-QAM at 64-GBd (1024 Gb/s gross data rate), respectively. It can be clearly observed that the NLPD outperforms the LPD in all three systems whilst exhibiting a similar behavior. At the small DA gain settings (<75), the system performance is mainly limited by the OSNR, resulting in similar results for both linear and nonlinear DPD methods. For gain settings ≥75, the nonlinear distortions produced by the DAs and modulator cause severe performance degradations, and limit the systems using LPD. Systems employing NLPD in contrast prove to be more resilient to such nonlinear distortions and still show almost the same performance up to the gain of 120. Ideally, the NLPD systems would maintain the same performance even for higher gain values. However, it is observed that the system performance starts degrading for the gain settings >120. This might be attributed to the limited DAC resolution (a nominal resolution of 8 bits and ~4.5 effective number of bits), which is even more restricting for highly nonlinearly predistorted signals in general due to the larger peak-to-average power ratio.

Conclusions

We propose a DSP scheme that systematically characterizes and mitigates the linear and nonlinear distortions caused by a high bandwidth integrated optical transmitter module specifically designed for 400G systems. The capability to identify and linearize such integrated modules, even considering high DA gain settings, was demonstrated for 64-GBd 64-QAM signals. It was shown that both the system performance and the transmitter output power and hence the transmitter OSNR can significantly be increased using the proposed method. The effectiveness of this identification and linearization process was further verified for systems up to 1024 Gb/s gross data rate (256-QAM at 64-GBd).

Acknowledgements

This work has been funded by German Bundesministerium für Bildung und Forschung (BMBF) under the Celtic Project SENDATE Secure-DCI (16KIS0479), SPEED (13N13748) and OptiCON (16KIS0990).

References

[1] F. Buchali et al., "1.52 Tb/s Single Carrier Transmission Supported by a 128 GSa/s SiGe DAC," 2020 Optical Fiber Communications Conference and Exhibition (OFC), San Diego, CA, USA, 2020, pp. 1-3.

[2] D. Rafique et al., "Digital Preemphasis in Optical Communication Systems: On the DAC Requirements for Terabit Transmission Applications," in Journal of Lightwave Technology, vol. 32, no. 19, pp. 3247-3256, 1 Oct.1, 2014, doi: 10.1109/JLT.2014.2343957.

[3] A. Napoli et al., "Novel digital pre-distortion techniques for low-extinction ratio Mach-Zehnder modulators," 2015 Optical Fiber Communications Conference and Exhibition (OFC), Los Angeles, CA, 2015, pp. 1-3, doi: 10.1364/OFC.2015.Th3G.1.

[4] D. Sadot et al., "Digital Pre-Compensation Techniques Enabling Cost-Effective High-Order Modulation Formats Transmission," in Journal of Lightwave Technology, vol. 37, no. 2, pp. 441-450, 15 Jan.15, 2019, doi: 10.1109/JLT.2018.2888941.

[5] P. W. Berenguer et al., "Nonlinear Digital Pre-distortion of Transmitter Components," in Journal of Lightwave Technology, vol. 34, no. 8, pp. 1739-1745, 15 April15, 2016, doi: 10.1109/JLT.2015.2510962.

[6] OIF Forum, "Implementation Agreement for High Bandwidth Coherent Driver Modulator (HB-CDM)", November 30, 2018 PDF online available at https://www.oiforum.com/wp-content/uploads/2019/01/OIF-HB-CDM-01.0.pdf

[7] G. Khanna, et. Al, "A Robust Adaptive Pre-Distortion Method for Optical Communication Transmitters," in IEEE Photonics Technology Letters, vol. 28, no. 7, pp. 752-755, 1 April1, 2016, doi: 10.1109/LPT.2015.2509158.

[8] G. Khanna et al., "A memory polynomial based digital pre-distorter for high power transmitter components," 2017 Optical Fiber Communications Conference and Exhibition (OFC), Los Angeles, CA, 2017, pp. 1-3.

[9] M. Kuschnerov et al., "Data-aided versus blind single-carrier coherent receivers," in IEEE Photon. Journal, vol. 2, no. 3, pp. 387–403, 2010. doi: 10.1109/JPHOT.2010.2048308

[10] R. Elschner et al., "Improving Achievable Information Rates of 64-GBd PDM-64QAM by Nonlinear Transmitter Predistortion," 2018 Optical Fiber Communications Conference and Exposition (OFC), San Diego, CA, 2018, pp. 1-3.

[11] R. Elschner et al., "Experimental demonstration of a format-flexible single-carrier coherent receiver using data-aided digital signal processing," vol. 20, no. 27, pp. 28786-28791, 2012. doi: https://doi.org/10.1364/OE.20.028786.

[12] H. Cheng et al., "Experimental demonstration of pilotsymbols-aided cycle slip mitigation for qpsk modulation format," in Proc. OFC, paper Th4D.1, San Francisco, CA, USA, 2014.

[13] C. Fludger et al., "Transmitter impairment mitigation and monitoring for high baud-rate, high order modulation systems", Tu.2.A.2, 2016.

[14] B. Szafraniec, et al., "Polarization demultiplexing in Stokes space," Opt. Express 18, 17928-17939 (2010).

[15] M. Selmi, et al., "Accurate digital frequency offset estimator for coherent PolMux QAM transmission systems," 2009 35th European Conference on Optical Communication, Vienna, 2009, pp. 1-2.

[16] R. D. Nowak, "Penalized least squares estimation of Volterra filters and higher order statistics," in IEEE Transactions on Signal Processing, vol. 46, no. 2, pp. 419-428, Feb. 1998, doi: 10.1109/78.655426.

[17] C. Eun et al., "A new Volterra predistorter based on the indirect learning architecture," in IEEE Transactions on Signal Processing, vol. 45, no. 1, pp. 223-227, Jan. 1997, doi: 10.1109/78.552219.